Insights About CHAPS Aggregation Obtained by Spin Label EPR Spectroscopy

Pablo M. Rodi, María D. Bocco Gianello & Ana M. Gennaro

Applied Magnetic Resonance

ISSN 0937-9347
Volume 45
Number 12

Appl Magn Reson (2014) 45:1319-1332
DOI 10.1007/s00723-014-0604-9

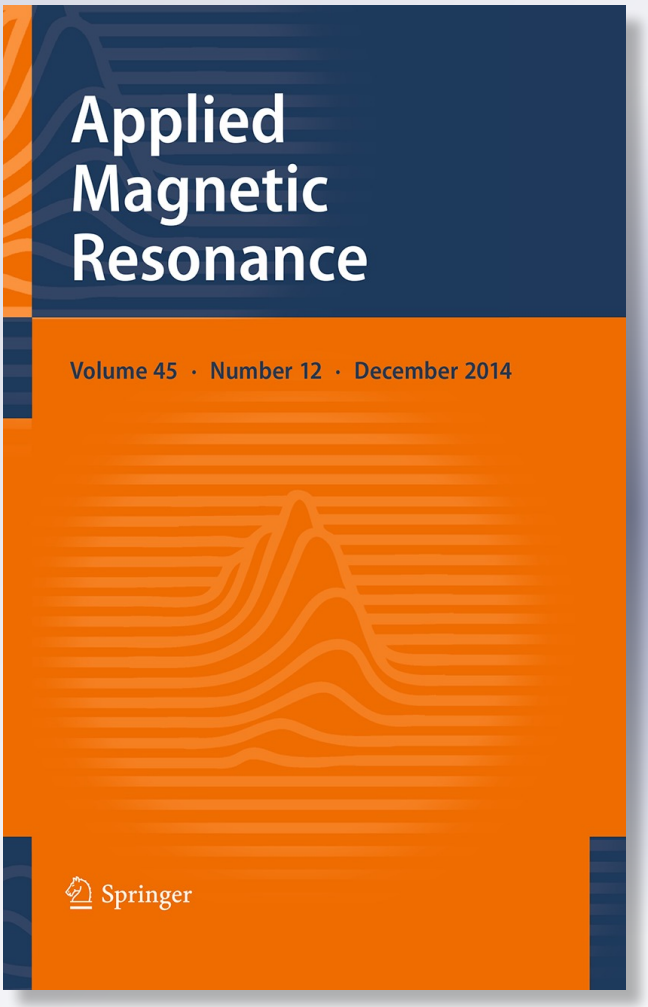

Springer

Appl Magn Reson (2014) 45:1319–1332
DOI 10.1007/s00723-014-0604-9

Applied
Magnetic Resonance

Insights About CHAPS Aggregation Obtained by Spin Label EPR Spectroscopy

Pablo M. Rodi · María D. Bocco Gianello · Ana M. Gennaro

Received: 28 July 2014 / Published online: 30 September 2014

Abstract CHAPS is a zwitterionic surfactant derivative of bile salts, widely used in membrane protein isolation. While some studies regarding CHAPS self-aggregation suggest continuous increase in micelle size at increasing CHAPS concentration, other works point to the existence of two definite micelle types. In this work, stearic acid spin labels (5, 12, or 16-SASL) were added to CHAPS solutions to obtain information about the micellar structure using electron paramagnetic resonance spectroscopy. The spectra of 12-SASL were processed using Principal Factor Analysis, and at all concentrations they could be reproduced as linear combinations of only three fundamental spectra, the first one corresponding to free 12-SASL in aqueous solution. This fact suggests only two hydrophobic environments that host 12-SASL, assigned to primary and secondary CHAPS micelles. The relative populations of the label in each environment were obtained as a function of CHAPS concentration. Our results suggest barrel-shaped primary micelles with a minimum mean radius of 1.46 nm, and a critical micelle concentration $cmc_I = 4$ mM. Secondary micelles are formed by aggregation of primary ones, with $cmc_{II} = 10$ mM. They have several elongated hydrophobic pockets, with similar dimensions for all aggregate sizes. Our results contribute to the understanding of the mechanism of interaction of chain amphiphiles with CHAPS micelles.

Electronic supplementary material The online version of this article (doi:10.1007/s00723-014-0604-9) contains supplementary material, which is available to authorized users.

P. M. Rodi · M. D. Bocco Gianello · A. M. Gennaro (✉)
Departamento de Física, Facultad de Bioquímica y Ciencias Biológicas, Universidad Nacional del Litoral (UNL), Ciudad Universitaria, 3000 Santa Fe, Argentina
e-mail: ana.gennaro@santafe-conicet.gov.ar; ana.gennaro@ifis.santafeconicet.gov.ar

A. M. Gennaro
IFIS Litoral (CONICET-UNL), Güemes 3450, 3000 Santa Fe, Argentina

1 Introduction

Surfactants are essential tools for the study of biological membranes [1]. They are frequently used to solubilize proteins from cell membranes, and to investigate the interactions among membrane lipid components. To obtain a correct description of these phenomena, it is necessary to obtain information about the interactions among surfactant molecules in aqueous solutions, leading to self-aggregation and formation of micellar structures in different conditions.

The zwitterionic surfactant CHAPS (3-[(3-cholamidopropyl)dimethylammonio]-1-propanesulfonate), a derivative of bile salts (Fig. 1), is widely used in membrane protein solubilization. It is a peculiar surfactant, with a ring steroid-type chemical structure, similar to that of bile salts, having a hydrophilic concave side where three OH groups protrude, and a hydrophobic convex back [2–6]. Due to these features, CHAPS can be considered as a facial surfactant [7], and this characteristic can explain why the mechanism of CHAPS interaction with erythrocyte membranes differs significantly from that of Triton X-100 [8]. CHAPS also has a mobile tail containing a zwitterionic amido sulfobetaine group.

CHAPS is very effective at breaking protein–protein interactions, disaggregating protein complexes without affecting secondary or tertiary structures [9, 10]. In a recent electron paramagnetic resonance (EPR) study of a spin-labeled transmembrane β-strand of outer membrane protein A reconstituted in several surfactants [11], it was shown that the protein-CHAPS interface is very different than that of straight chain amphiphiles, and there are significant packing defects between the protein and CHAPS. Although molecular packing in a protein/surfactant complex is expected to differ to that of a pure surfactant micelle, the study of surfactant self-assembled structures can give information about its packing preferences that could affect its interactions with proteins and lipids.

Several studies have been recently performed regarding CHAPS self-assembly. Using isothermal titration calorimetry, Kroflic et al. [12] concluded that, similar to bile salts, CHAPS micelles are small (5–6 monomers) and loose aggregates, leaving a large amount of water molecules in contact with the hydrophobic regions of the surfactant molecules. Lipfert et al. [13], using SAXS in a wide variety of surfactants, reported for CHAPS micelles the singularity of lacking the scattering contrast characteristic of well-delimited hydrophobic and hydrophilic regions. Their

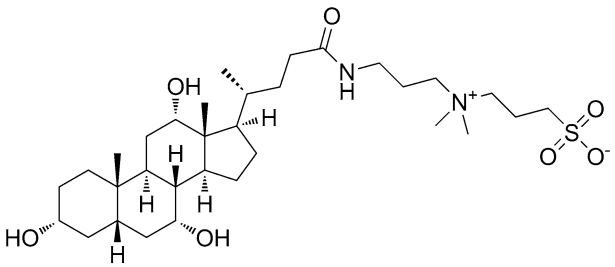

Fig. 1 Molecular structure of the surfactant CHAPS

results also point to a continuous increase in micelle size at increasing CHAPS concentration [13]. A similar conclusion was obtained in a recent molecular dynamics study [14]. On the other side, ^{1}H NMR studies [15, 16] provided evidences of the formation of a second type of micellar "staggered" aggregates at high CHAPS concentration.

Electron paramagnetic resonance spectroscopy with spin labels has been used in several studies to investigate the self-assembly process and the properties of surfactant micelles [17–19]. In the present paper, we use EPR spectroscopy to study CHAPS solutions in which low amounts of the liposoluble spin labels *n*-SASL, bearing a stable free radical in a nitroxide moiety at the position $n = 5$, 12 or 16 of a stearic acid chain, were added. From the EPR spectra, we obtain parameters related to the nitroxide dynamics that contribute to the characterization of the micellar structures, and the changes appearing at increasing CHAPS concentration.

2 Experimental Section

2.1 Materials

The zwitterionic surfactant CHAPS (3-[(3-Cholamidopropyl)dimethylammonio]-1-propanesulfonate) was from AMRESCO LLC (Solon, USA). The non-ionic surfactant Triton X-100, the liposoluble spin labels *n*-doxyl-stearic acid positional isomers (*n*-SASL, $n = 5$, 16) were from Sigma (St. Louis, USA), and 12-SASL from Toronto Research Chemicals (North York, ON, Canada). Solvents, inorganic salts, and all other chemicals were of the highest available purity.

2.2 Spin Labeling

The liposoluble *n*-doxyl-stearic acid spin labels (*n*-SASL; $n = 5$, 12 or 16) were incorporated by room temperature incubation to the surfactant solutions. The final spin label/surfactant molar ratio was always less than or equal to 1 % to minimize disturbances in the behavior of CHAPS, and to avoid line broadening effects in the EPR spectra. Briefly, an adequate volumen of an ethanolic stock solution of each spin label was deposited at the bottom of test tubes, and the solvent was evaporated. Aliquots of different surfactant concentrations in isotonic Tris saline buffer (TBS, pH 7.4) were added. The samples were incubated for 30 min at room temperature, and afterward suctioned into glass capillaries; subsequently, flame sealed in one end and put into 4-mm quartz tubes.

2.3 EPR Spectroscopy

Electron paramagnetic resonance spectra were acquired at 22 ± 1 °C at 9.8 GHz (X-band) in a Bruker EMX-Plus spectrometer. In a first, qualitative analysis, we evaluated the apparent order parameter S_{app} [20]. This parameter is related to both the dynamics and the angular amplitude of motion of the *z*-axis of the nitroxide molecular frame, pointing along the unpaired electron p-orbital, and its values lie in

the range $0 < S_{app} < 1$. We also evaluated the isotropic hyperfine parameter a_0, indicative of the polarity of the nitroxide environment [20], from the almost isotropic spectra of 16-SASL. Details of the calculations are included in the Supplementary Material. A more detailed analysis of the spectra of 12-SASL at several CHAPS concentrations was performed using Principal Factor Analysis (PFA) (Sect. 2.4) and the Easyspin software [21].

2.4 Analysis of the EPR Spectra as a Function of CHAPS Concentration

To study the changes in CHAPS aggregation when surfactant concentration is increased, we apply PFA [22] to a set of twenty EPR spectra of 12-SASL in CHAPS solutions of concentrations ranging between 0.8 and 162 mM. The spin label to surfactant molar ratio was always less than or equal to 1 %. Spectra were normalized to unit peak-to-peak amplitude, and corrected for the slight differences in resonance frequencies among samples.

The PFA method is very reliable to determine the number and the characteristics of the independent components giving rise to the evolution of a series of spectra involving a linear behavior [23]. It considers the set of measured spectra as vectors belonging to a vectorial space (the "factor space"), and it allows one to determine the number N of components of the basis of this vectorial space. With additional hypothesis and physical criteria, the method also allows one to identify the independent fundamental spectra that confirm this basis. Once these fundamental spectra have been identified, least squares fittings can be performed, to reproduce each experimental spectrum of the series as a linear combination of the fundamental ones. The coefficients of these linear combinations represent the weight of each of the components in the composite spectrum at the corresponding surfactant concentration. More details of the analysis are included in the Supplementary Material section.

3 Results and Discussion

3.1 EPR Spectra of Liposoluble Spin Labels in CHAPS Micelles at Two Surfactant Concentrations

The nitroxide EPR spectrum is sensitive to order/dynamics of its environment [20, 21]. The liposoluble spin labels *n*-SASL bear a nitroxide moiety attached to the *n*th carbon of a stearic acid molecule. Thus, when they are incorporated to "conventional" micellar structures (i.e., those having a hydrophobic core surrounded by a polar shell), 5-SASL, with the nitroxide in the nearest position to the stearic acid polar end, senses the outer portion of the hydrophobic region, near the polar moieties, while 16-SASL senses the innermost part of the hydrophobic core. A "fluidity gradient", consisting of monotonically decreasing values of the apparent order parameter S_{app}, is observed in these "conventional" micelles, indicating more restricted motions near the polar heads, and increased degrees of freedom for 12- and 16-SASL, due to the increased rate of trans-gauche

isomerizations of the stearic acid chains in a more fluid environment [20]. This is the case of Triton X-100 micelles, but it will be shown that CHAPS has a drastically different behavior.

Electron paramagnetic resonance spectra of spin-labeled CHAPS micelles prepared at two different concentrations (29 and 162 mM) are shown in Fig. 2a and b. It can be seen that for a same label, the spectra differ at the two concentrations, in a subtle way for 5- and 16-SASL, but very clearly for 12-SASL.

Apparent order parameters S_{app}, calculated from the spectra of Fig. 2 as described in the Supplementary Material section, are plotted in Fig. 3 as a function of the position of the nitroxide moiety in the stearic acid chain. S_{app} values for Triton X-100, a surfactant having a "conventional" micelle structure [24], are also included in Fig. 3 for comparison. The S_{app} values for Triton X-100 show the expected "fluidity gradient", i.e., they decrease monotonously as the position of the nitroxide radical in the stearic acid chain increases. However, the unexpected result found in CHAPS is the maximum (and unusually high) value of S_{app} for 12-SASL, indicating that this label is strongly immobilized, and deviating from the "normal" fluidity gradient. This tendency indicates that the hydrophobic environment hosting stearic acid spin labels in CHAPS micelles imposes large mobility restrictions to 12-SASL—that bears the nitroxide at the middle portion of stearic acid chain—but allows higher mobility to 5- and 16-SASL, having the nitroxide ring near both the ends of the stearic acid chain. A similar tendency was reported by Kawamura et al. [19] for SASL in bile salt micelles.

These results can be explained if the hydrophobic regions capable to host stearic acid spin labels in CHAPS micelles are narrow enough to not allow *trans-gauche* isomerizations of the stearic acid chain portion inside them, and short enough to host only 9–10 carbon molecules of the chain. These regions are schematized as cylinders in Fig. 4 together with the SASL molecules. As it is expected that the more hydrophobic portions of the SASL are housed into the micelle hydrophobic regions, the mobility of the nitroxide ring of 12-SASL will be limited due to its proximity to the immobilized portion of the chain, leading to a high S_{app}. However, in the case of 5- and 16- SASL, the degrees of freedom of the chain portion that does not fit into the hydrophobic region will give high mobility to the nitroxide ring, thus explaining the low values of S_{app}.

Information related to water penetration can be obtained from the isotropic hyperfine splitting a_0, which depends on the polarity of the label environment [20], and can be determined from the almost isotropic spectra of 16-SASL, as shown in Figure S1b of the Supplementary Material. As instance, for 16-SASL free in aqueous solution, we obtained $a_0 = 15.9$ G, while in a non-polar medium as CCl_4, $a_0 = 14.4$ G. In TX-100 micelles, $a_0 = 14.6$ G, indicating low water penetration in the center of these conventional micelles. However, in the case of CHAPS, the hyperfine splitting a_0 is 15.0 G at 29 mM, and 14.9 G at 162 mM, indicating that 16-SASL is more exposed to water in CHAPS than in Triton X-100 micelles. This is also consistent with the proposed shape of the hydrophobic region.

These results point to a non-conventional structure of CHAPS micelles, having narrow hydrophobic "pockets" instead of a central hydrophobic core. Funasaki et al. [6] proposed micelles with a "back to back" association of seven CHAPS

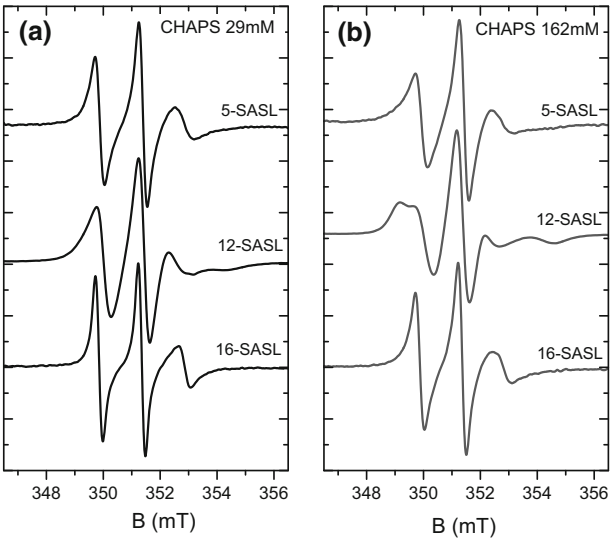

Fig. 2 EPR spectra of stearic acid spin labels in CHAPS solutions of two different concentrations

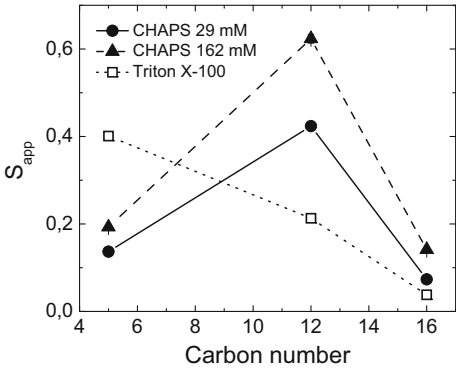

Fig. 3 Apparent order parameters obtained from EPR spectra of CHAPS micelles. The abscissa values represent the position of the nitroxide ring in the stearic acid chain. (lower values are closer to the polar end). Results obtained in Triton X-100 "conventional" micelles are also included for the sake of comparison. For CHAPS, the non-monotonic dependence of S_{app} upon carbon number suggests a non-conventional micelle structure

molecules, compatible with a barrel structure. In this way, the hydrophobic convex sides of the ring structure would be pointing to the inside, and the concave sides bearing the OH groups would be facing the aqueous environment. There is also consistence with the results of Kroflic et al. [12], who described CHAPS micelles as loose structures with high water penetration, and with those of Lipfert et al. [13], showing the absence of separate hydrophobic and polar regions. However, our results do not support the proposed micelle shape of Qin et al. [15, 16].

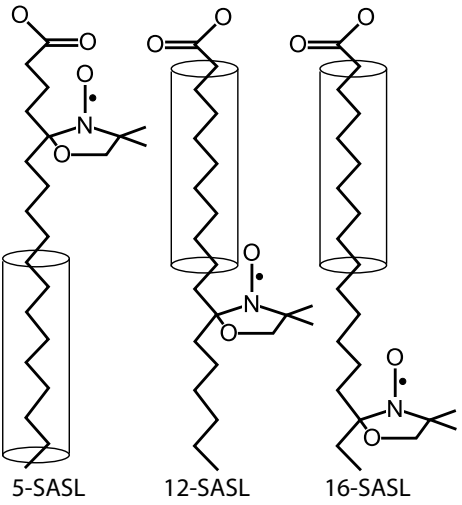

Fig. 4 A scheme showing the spin labels *5-*, *12-*, and *16-SASL*, together with a simplified model of the hydrophobic regions inside CHAPS micelles, depicted as cylinders

On the other side, the changes in the EPR spectra at increasing CHAPS concentrations, especially significant in the case of 12-SASL (Fig. 2), deserve to be analyzed in detail. This task is detailed in the next section.

3.2 EPR Spectra of 12-SASL in CHAPS Solutions at a Wide Range of Surfactant Concentrations

To analyze in detail the spectral changes as a function of CHAPS concentration, and taking into account that the more striking changes were seen in the 12-SASL spectra, twenty CHAPS solutions in the range 1.6–162.6 mM in TBS were prepared, including a minimum amount of 12-SASL (spin probe to surfactant molar ratio less or equal to 1 %), and their EPR spectra were obtained. Figure 5 shows a selection of the spectra.

All the spectra taken at concentrations lower than 4 mM show three narrow lines, indicating high mobility, and are coincident with the spectrum of 12-SASL in aqueous solution. The first spectrum of Fig. 5 is representative of this case. This is the expected behavior for surfactant concentrations below the critical micellar concentration (cmc), where only monomers are present, and there are no hydrophobic regions to host 12-SASL. As CHAPS concentration increases, wider spectral structures appear superimposed; the narrow lines gradually decrease, and eventually disappear. These facts indicate a decrease in the mobility of 12-SASL, consisting with its incorporation to micellar structures. In turn, the wider spectra also suffer a continuous change at increasing concentrations (Fig. 5).

Taking into account these results, the following question arises: are the spectra of Fig. 5 indicative of a gradual change of the spin label environment, or rather they represent the superposition of a discrete number of environments whose relative weights change with CHAPS concentration?

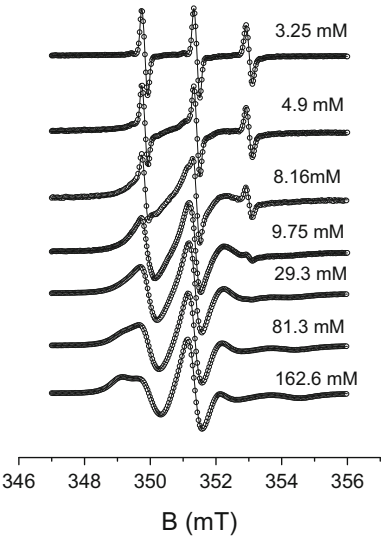

Fig. 5 Selected spectra of 12-SASL in CHAPS solutions showing the changes as surfactant concentration increases. *Points* correspond to experimental spectra, and *full lines* are least squares fit with linear combinations of the three fundamental spectra identified by principal factor analysis (see below). For the sake of comparison, peak-to-peak amplitudes of the central lines have been normalized. (the whole set of spectra is included in the Supplementary Material section)

3.2.1 Principal Factor Analysis

To address the question of the previous paragraph, we analyzed the set of twenty EPR spectra of 12-SASL in CHAPS solutions of different concentrations with the method of PFA and target transformation [22, 23]. The method and the procedure are briefly described in Sect. 2.4 and in the Supplementary Material. This analysis leads us to determine that all the experimental spectra could be reproduced as linear combinations of only three fundamental spectra, shown in Fig. 6, and labeled as Components 1, 2, and 3. The coefficients of the linear combinations that best reproduce the experimental spectra were calculated by least squares analysis, and are plotted in Fig. 7 as a function of CHAPS concentration. These coefficients represent the relative weight of each fundamental component to the experimental EPR spectrum.

The correctness of our analysis is supported by the fact that each one of the 20 experimental spectra can be reconstructed as a sum of the three independent components with their corresponding weights, with an excellent agreement with the experimental data. In Fig. 5, we had included seven reconstructed spectra (full lines) together with their respective experimental spectra. The whole set of spectra with their fits is included in the Supplementary Material, Fig. S3a and b.

Therefore, our results indicate that the changes in the EPR spectra at increasing CHAPS concentrations shown in Fig. 5 are not due to a continuous change of the environmental conditions, but instead 12-SASL senses only three different environments in the whole concentration range, whose occupation changes as a function of concentration. Moreover, we obtained the shape of each of the fundamental spectra corresponding to these environments, and the spectral weight they have at each of the CHAPS concentrations.

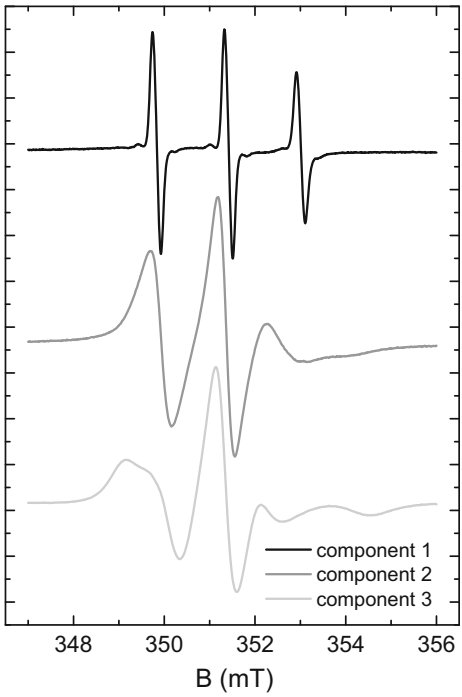

Fig. 6 The three physically meaningful EPR spectra corresponding to the independent components obtained from principal factor analysis. The normalized spectrum of 12-SASL at any of the studied CHAPS concentrations can be well reproduced by linear combinations of these three components, with the weights displayed in Fig. 7

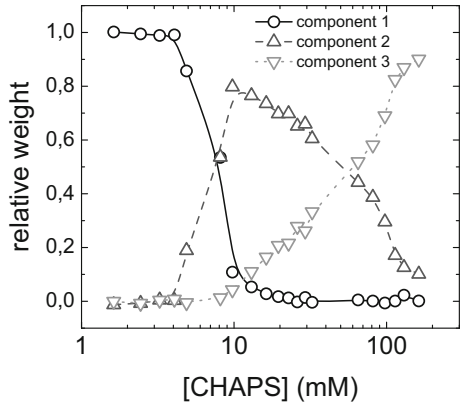

Fig. 7 Relative weights obtained by least squares fit of linear combinations of the spectra of Fig. 6 to the experimental EPR spectra of 12-SASL at each CHAPS concentration. *Lines* are only an aid to the eye. The cmc values pointed to by arrows will be discussed in Sect. 3.2.2

The next step is to analyze these fundamental spectra, to propose a physical interpretation of each one of the environments sensed by 12-SASL.

3.2.2 Analysis of Each Spectral Component

The spectrum of Component 1 (Fig. 6) is typical for a highly mobile spin label tumbling isotropically in a low viscosity medium. The hyperfine splitting a_0 is

(15.9 ± 0.1) G, consistent with the experimental value measured for 12-SASL in water. In the isotropic mobility regime, the EPR spectrum depends only on the rotational correlation time of the labeled molecule [20]. A least squares fit with the Easyspin software [21], using the routines for fast isotropic motion, yielded a rotational correlation time $\tau_{c1} = 0.19$ ns. The inspection of the relative weights plotted in Fig. 7 shows that Component 1 is the only present up to 4 mM CHAPS, indicating that up to that surfactant concentration, the spin label senses only an aqueous environment in which it is rotating isotropically, i.e., no CHAPS micelles are still present. No change in the spectral widths of the individual lines of the EPR experimental spectra is observed in this range (see all the spectra in this range in Fig. S3a in the Supplementary Material), indicating that the spin label is not forming micelles by itself, which would lead to exchange widening and eventually collapse of the spectral lines. The absence of spectral changes in this concentration range also indicates that no relevant interactions appear between 12-SASL and CHAPS monomers. The gradual reduction of the weight of Component 1 for CHAPS concentrations higher than 4 mM (in the range of reported CHAPS cmc values [9, 10, 15, 16]), at the expenses of the increased weight of the more immobilized Component 2 (Fig. 7) suggests the partition of 12-SASL molecules between the aqueous solution and a "primary micelle" type, appearing at 4 mM CHAPS (cmc_I).

As the EPR spectrum of Component 2 is no longer indicative of high mobility, it was analyzed by taking into account the "slow motion" behavior [25], using the Easyspin routine *Chili* [21], based on the programs developed by Freed and coworkers [25]. These programs are able to separate effects of dynamics (correlation times) and order (order parameter). The best fit of this spectrum yields order parameter $S = 0$, and an isotropic rotational correlation time $\tau_{c2} = (3.15 \pm 0.04)$ ns. Figure 8a shows the spectrum together with the fit.

Finding an isotropic spectrum in primary micelles seems inconsistent with the previous results indicating that 12-SASL is hosted in an elongated region with its movements highly hindered, leading to expect a spectrum showing mobility restrictions. The inconsistency is removed if we assume that the detected isotropic spatial dynamics is that of the whole primary micelles, rotating isotropically with a correlation time fast enough to wipe out any internal anisotropy. Then, considering that the correlation time calculated from the fit of the EPR spectrum of Component 2 corresponds to the whole micelle, we can make an estimation of the primary micelle size using the Debye–Stokes–Einstein relationship $\tau_{c2} = \frac{V_h \eta}{kT}$, where V_h is the hydrodynamic volume of the micelle and η is the viscosity of the medium. We obtain a mean hydrodynamic radius of (1.46 ± 0.01) nm that should be considered as a lower bound for the mean radius of primary CHAPS micelles. This value is in excellent agreement with the experimental results obtained by Qin et al. [15, 16], and Lipfert et al. [13], and it is in the range of the micelle radii calculated by Herrera et al. [14] using molecular dynamics. These coincidences provide support to our hypothesis that spectral Component 2 mainly reflects the dynamics of the whole primary micelles. Also, primary micelle formation is detected at a cmc (cmc_I, 4 mM) in the range of published data obtained in pure CHAPS [9, 10, 15, 16], suggesting that 12-SASL perturbations on CHAPS aggregation behavior are

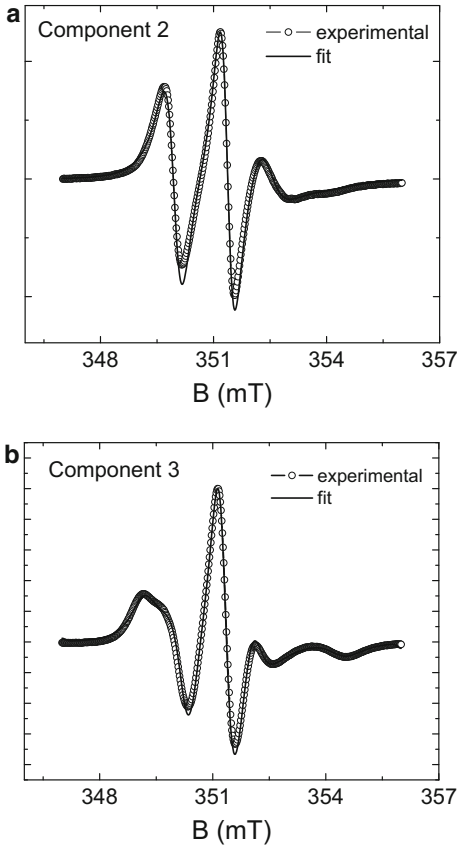

Fig. 8 **a** *Circles*, second independent spectrum (*Component 2*) obtained from PFA, and assigned to 12-SASL in primary micelles. *Full line* is the fit assuming isotropic rotation of the spin label; **b** *circles*, third independent spectrum (*Component 3*), assigned to 12-SASL in secondary micelles. *Full line* is the fit assuming a restricted rotation. The fit parameters are reported in the text (Sect. 3.2.2)

negligible, and that our results are representative of the behavior of pure CHAPS micelles.

As seen in Fig. 7, the third spectral component appears around 10 mM CHAPS, and its relative weight increases slowly with CHAPS concentration, at the expenses of the decrease of Component 2. The best fit of the EPR spectrum of Component 3 with the Easyspin software yields an order parameter $S = 0.33$, and rotational correlation times $\tau_{c3\perp} = 4.8$ ns, $\tau_{c3//} = 10^{-2}$ ns. Thus, 12-SASL dynamics is no longer isotropic, and it can be described as fluctuations of the angle between the molecular z-axis (direction of the nitroxide p-orbital) and its most probable orientation [20], with a characteristic time of 4.8 ns, and a maximum angle aperture of 63°, estimated from the order parameter $S = 0.33$ [20]. (The low value of $\tau_{c3//}$ indicates very fast rotation of the spin label around its long axis that does not affect the spectral features [20]).

Figure 8b shows the spectrum of Component 2 together with the fit. It is reasonable to propose that this spectrum corresponds to 12-SASL inserted into a second micelle type having a $cmc_{II} = 10$ mM. Note, in Fig. 7, that the spectral changes at concentrations higher than cmc_{II} are very well described by an increasing

weight of Component 3, correlated with the decrease of Component 2 (primary micelles).

It has been shown that in bile salts, which have structural similarities with CHAPS, polydisperse secondary micelles are formed by aggregation of primary ones (Small [26], Partay et al. [27]). Also, molecular dynamics simulations [14] have shown that the larger CHAPS micelles have a grain-like heterogeneity, with several hydrophobic pockets. The presence of only one kind of EPR spectrum attributed to 12-SASL in secondary micelles, despite the polydispersity and the expected increase in micelle size at increasing concentrations reported by Lipfert et al. [13]. can be explained if we assume that CHAPS secondary micelles are also formed by the aggregation of primary ones, as proposed for bile salts [26, 27]. In this way, the hydrophobic cavities able to host 12-SASL would have roughly the same shape and dimensions, regardless the size of secondary micelles. An extra condition is that the rotational dynamics of any secondary micelle must be slow enough to not affect the EPR spectrum of an attached spin label. As explained in detail in the Supplementary Material, from the radius estimated for primary micelles, the coalescence of 4 or more of them is needed to fulfill this requirement. Smaller secondary micelles, formed by 2 or 3 primary micelles, are thus expected to give different EPR spectra. However, our experiments are well described by only two fundamental spectra attributed to 12-SASL in micelles. Thus, we are led to conclude that secondary micelles are formed preferentially by the aggregation of 4 or more primary micelles, and/or that the structures formed by the coalescence of just 2 or 3 of them cause a negligible contribution to the EPR spectra of CHAPS solutions.

3.3 Concluding Remarks

There is not established consensus regarding the shape of the supramolecular structures formed by CHAPS upon self-assembly. To obtain additional insights, we performed EPR experiments adding small amounts of stearic acid spin labels to CHAPS solutions. According to our results, primary micelles form at about 4 mM, in coincidence with the range of critical micellar concentrations reported in pure CHAPS, and have typical dimensions of 1.46 nm. This size is consistent with those obtained in the molecular dynamics simulations, and the proposed shape of the hydrophobic region is consistent with barrel type aggregates, like those proposed by Funasaki et al. [6] for CHAPS, and Kawamura et al. [19] for bile salts. There is also consistence with the results of Kroflic et al. [12], who described CHAPS micelles as loose structures with high water penetration, and with those of Lipfert et al. [13], showing the absence of separate hydrophobic and polar regions. However, our results do not support the proposed spherical micelle shape of Qin et al. [15, 16].

Secondary micelles are formed at CHAPS concentrations above 10 mM by aggregation of primary micelles, thus having several hydrophobic pockets of similar size and shape. Re-orientational dynamics of aggregates formed by more than four primary micelles is slow enough to not affect the shape of the EPR spectrum, resulting in only one spectral component (Component 3) for these secondary micelles.

A final note of caution should be added, as we cannot forget that we are sensing only the micelles into which a spin label molecule was incorporated, and that stearic acid spin labels are themselves amphiphiles. Thus, it might be possible that the 12-SASL molecule generates by itself changes in the structure of the hydrophobic pockets of CHAPS micelles. However, the cmc_I determined from our experiments is in the range of the values measured in pure CHAPS systems, suggesting that the disturbances caused by 12-SASL are minimal. To test the validity of these assumptions, molecular dynamics simulations of CHAPS micelles containing stearic acid spin labels are planned.

Our results contribute to the understanding of the mechanism of interaction of chain amphiphiles with CHAPS micelles. This information could be relevant for the solubilization of membrane lipids in aqueous solutions for ^{31}P-NMR studies, where detergent micelles of small size are essential to avoid lipid–lipid interactions and to ensure high mobility, leading to high spectral resolution [28]. This task is usually performed with sodium cholate, but according to our results, CHAPS at 10 mM concentration, where primary micelles predominate, could be a good candidate to perform these kinds of studies.

Acknowledgments This work was supported by CONICET and Universidad Nacional del Litoral. AMG is a researcher of CONICET. PMR had a scholarship from CONICET during part of the execution of this work. We thank Dr RR Koropecki for kindly allowing us the use of his PFA programs, and providing useful advice, and Dr Raúl Urteaga for helpful discussions.

References

1. H. Heerklotz, Quarterly Rev Biophys **41**, 205–264 (2008)
2. L.M. Hjelmeland, Proc Natl Acad Sci USA **77**, 6368–6370 (1980)
3. C.E. Giacomelli, A.W.P. Vermeer, W. Norde, Langmuir **16**, 4853–4858 (2000)
4. K. Lunkenheimer, G. Sugihara, M. Pietras, Langmuir **23**, 6638–6644 (2007)
5. R.E. Stark, P.D. Leff, S.G. Milheim, A. Kropf, J Phys Chem **88**, 6063–6067 (1984)
6. N. Funasaki, M. Fukuba, T. Hattori, S. Ishikawa, T. Okunoa, S. Hirota, Chem Phys Lipids **142**, 43–57 (2006)
7. J. Boekhoven, P. van Rijn, J.H. van Esch, in *Supramolecular chemistry: from molecules to nanomaterials*, vol. 7, ed. by P.A. Gale, J.W. Steed (Wiley, USA, 2012), pp. 3377–3394
8. P.M. Rodi, M.D. Bocco Gianello, M.C. Corregido, A.M. Gennaro, Biochim Biophys Acta Biomembranes **1838**, 859–866 (2014)
9. L.M. Hjelmeland, D.W. Nebert, J.C. Osborne, Anal Biochem **130**, 72–82 (1983)
10. A. Chattopadhyay, K.G. Harikumar, FEBS Lett **391**, 199–202 (1996)
11. R.H. Flores Jiménez, D.M. Freed, D.S. Cafiso, J Phys Chem B **115**, 14822–14830 (2011)
12. A. Kroflic, B. Sarac, M. Bester-Rogac, Langmuir **28**, 10363–10371 (2012)
13. J. Lipfert, L. Columbus, V.B. Chu, S.A. Lesley, S. Doniach, J Phys Chem B **111**, 12427–12438 (2007)
14. F.E. Herrera, A.S. Garay, D.E. Rodrigues, J Phys Chem B **118**, 3912–3921 (2014)
15. X. Qin, M. Liu, D. Yang, X. Zhang, J Phys Chem B **114**, 3863–3868 (2010)
16. X. Qin, M. Liu, X. Zhang, D. Yang, J Phys Chem B **115**, 1991–1998 (2011)
17. M.A. Bahri, M. Hoebeke, A. Grammenos, L. Delanaye, N. Vandewalle, A. Seret, Coll Surf A Physicochem Eng Asp **290**, 206–212 (2006)
18. A. Lewinska, M. Witwicki, U. Bazylinska, A. Jezierski, K.A. Wilk, Coll Surf A Physicochem Eng Asp **442**, 34–41 (2014)

19. H. Kawamura, Y. Murata, T. Yamaguchi, H. Igimi, M. Tanaka, G. Sugihara, J. Kratohvil, J Phys Chem **93**, 3321–3326 (1989)
20. O.H. Griffith, P. Jost, in *Spin labeling: theory and applications*, ed. by L.J. Berliner (Academic Press, New York, 1976), p. 454
21. S. Stoll, A. Schweiger, J Magn Reson **178**, 42–55 (2006)
22. E.R. Malinowski, D.G. Howery, *Factor analysis in chemistry* (Wiley, New York, 1980)
23. R.R. Koropecki, F. Alvarez, R. Arce, J Appl Phys **69**, 7805–7811 (1991)
24. R.J. Robson, E.A. Dennis, J Phys Chem **81**, 1076–1078 (1977)
25. D.J. Schneider, J.H. Freed, in *Biological magnetic resonance*, vol. 8, ed. by L.J. Berliner, et al. (Plenum Press, New York, 1989), pp. 1–76
26. D.M. Small, in *The Bile Acids Chemistry, Physiology, and Metabolism*, vol. 1, ed. by P.P. Nair, D. Kritchevsky (Plenum Press, New York, 1971). (Ch. 8)
27. L.B. Partay, P. Jedlovsky, M. Sega, J Phys Chem B **111**, 9886–9896 (2007)
28. A. Puppato, D.B. DuPre, N. Stolowich, M.C. Yappert. Chem Phys Lipids **150**, 176–185 (2007)